Table II. ^{1}H NMR of $B_{10}H_{14}$ in Various Solvents

solvent	atom positions				
	H(1,3)	H(6,9)	H(5,7,8,10)	H(2,4)	H(μ)
C_6D_6	4.12[a] (141)[b]	3.51 (157)	3.10 (158)	1.05 (157)	−1.21
CD_2Cl_2	3.87[c]	3.64[c]	3.11[c]	0.63 (157)	−2.07
THF-d_8	3.76[c]	3.58[c]	3.03[c]	0.58 (155)	−1.73
$(CD_3)_2CO$	3.83[c]	3.57[c]	3.03[c]	0.58 (154)	−1.55
CD_3CN	3.82[c]	3.53[c]	2.99[c]	0.55 (155)	−1.92

[a] Chemical shift in δ from Me_4Si. [b] ^1H_t-^{11}B coupling in Hz. [c] Coupling constant values were not determined due to overlap of hydrogen resonances, but they are on the same order of magnitude as those determined in C_6D_6 solution.

variations for other hydrogen resonance positions, as shown in Table II and Figure 4.

B(2,4)–B(6,9) Coupling. In low-polarity low molecular weight solvents such as *n*-butane and *n*-pentane, the ^{11}B NMR spectra of $B_{10}H_{14}$ display evidence of substantial fine structure in the B(6,9) resonance (Figure 5). Upon line narrowing, each half of the B(6,9) resonance exhibits eight clean resonances. In the line-narrowed $^{11}B\{^1H\}$ NMR spectrum the B(6,9) resonance is a 1:1:1:1 quartet with $J_{B(2,4)-B(6,9)} = 18 \pm 1$ Hz. The B(6,9) resonance is then a doublet of triplets of quartets, with coupling constants of 160 ± 2 (^{11}B–H_t), 40 ± 2 (^{11}B–H_b), and 18 ± 2 (^{11}B–^{11}B), respectively, identified in Figure 1.

Overlap of the triplet of quartets produces the approximate 1:1:3:3:3:3:1:1 appearance of each half of the line-narrowed resonance. The coupling is clearly visible in the B(6,9) resonance, as the boron atoms in these positions are bonded to only three other boron atoms and the bonding of two of them is via bridging hydrogen atoms. The B(2,4) atoms, on the other hand, are each adjacent to five other boron atoms in the molecule and, as a result, do not exhibit any resolvable fine structure, even upon substantial line narrowing. ^{11}B–^{11}B coupling has been observed in a number of small boron hydrogen clusters and typically exhibits a coupling constant of about 20 Hz.[4a,b,5]

The observation of coupling beyond that due to ^{11}B–^1H_t in $B_{10}H_{14}$ was recorded by Schaeffer[4a] who was able to resolve a doublet of quartets but indicated that this was a complex pattern and did not define it further. Odom and Ellis[4b] reported a $^{11}B(2,4)$–$^{11}B(6,9)$ coupling constant of 18.7 Hz from a $^{11}B\{^1H\}$ 32.1-MHz line-narrowed NMR spectrum in CS_2 solution.

In low-polarity high molecular weight solvents such a *n*-octane and C_6F_6 the ^{11}B–^{11}B coupling appears unresolvable. This suggests that the viscosity of the solvent is affecting the $B_{10}H_{14}$ correlation time, τ_R, such that the coupling cannot be observed on the NMR time scale. A recent study[6] on relaxation times in $B_{10}H_{14}$ in perdeuteriotoluene indicated that T_1 for ^{11}B depends only on τ_R when isotropic tumbling is occurring. It was demonstrated that as the temperature was raised, $T_1(^{11}B)$ also increased (and τ_R decreased). For quadrupolar nuclei that are interacting directly with only a few other nuclei, the effect of an increased T_1 may render fine structure observable. B(6,9), having only one direct ^{11}B–^{11}B interaction with B(2,4), shows the ^{11}B–^{11}B coupling in low-viscosity solvents or at higher temperatures. This temperature effect on the B(6,9) fine structure resolution occurs with a moderate temperature increase from 298 to 333 K for $B_{10}H_{14}$ in C_6D_6. The other boron positions in $B_{10}H_{14}$ interact with a larger number of nuclei in the molecule. These interactions give rise to more complex spin patterns, which are currently unresolved.

Acknowledgment. This work was supported in part by grants, including departmental grants for NMR facilities, from the National Science Foundation (D.F.G.). Support is also acknowledged from the SERC for a project grant and the use of the high-field NMR service at Edinburgh University (J. H.M.).

Registry No. $B_{10}H_{14}$, 17702-41-9; Me_4Si, 75-76-3; CD_2Cl_2, 1665-00-5; C_6F_6, 392-56-3; CS_2, 75-15-0; CD_3CN, 2206-26-0; THF, 109-99-9; *n*-butane, 106-97-8; *n*-pentane, 109-66-0; *n*-hexane, 110-54-3; octane, 111-65-9; cyclohexane, 110-82-7; benzene-d_6, 1076-43-3; acetone-d_6, 666-52-4.

(4) (a) Clouse, A. O.; Moody, D. C.; Rietz, R. R.; Roseberry, T.; Schaeffer, R. *J. Am. Chem. Soc.* **1973**, *95*, 2496. (b) Stampf, E. J.; Garber, A. R.; Odm, J. D.; Ellis, P. D. *J. Am. Chem. Soc.* **1976**, *98*, 6550.
(5) Weiss, R.; Grimes, R. N. *J. Am. Chem. Soc.* **1978**, *100*, 1401. Odom, J. D.; Ellis, P. D.; Walsh, H. C. *J. Am. Chem. Soc.* **1971**, *93*, 3529. Onak, T.; Leach, J. B.; Anderson, S.; Frisch, M. J.; Marynick, D. *J. Magn. Reson.* **1976**, *23*, 237. Lowman, D. W.; Ellis, P. D.; Odom, J. D.; *J. Magn. Reson.* **1972**, *8*, 289. Odom, J. D.; Ellis, P. D.; Lowman, D. W.; Gross, M. H. *Inorg. Chem.* **1973**, *12*, 95. Lowman, D. W.; Ellis, P. D.; Odom, J. D. *Inorg. Chem.* **1973**, *12*, 681. Astheimer, R. J.; Plotkin, J. S.; Sneddon, L. G. *J. Chem. Soc., Chem. Commun.* **1979**, 1108.
(6) Gibb, T. C.; Kennedy, J. D. *J. Chem. Soc., Faraday Trans. 2* **1982**, *78*, 525.

Contribution from the School of Chemistry,
The University of New South Wales,
Kensington NSW, Australia 2033,
and Department of Chemistry, The University of California,
Santa Barbara, California 93106

Observation of both Bridging and Chelating Modes of the 2-(2-Pyridyl)-1,8-naphthyridine Ligand (pynp) in a Single Dirhodium(II) Complex: X-ray Structure of $[Rh_2(pynp)_3Cl_2][PF_6]_2 \cdot CH_3CN$

A. T. Baker,*[1] Wayne R. Tikkanen,[2] William C. Kaska,[2]
and Peter C. Ford*[2]

Received October 5, 1983

Polydentate ligands have the capacity to bind metals in different modes utilizing some or all of the base sites. For example, 2-2(2-pyridyl)-1,8-naphthyridine (pynp) can act as

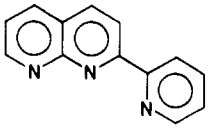

pynp

a bidentate chelating ligand in tris complexes with ruthenium(II)[3] or as a tridentate bridging ligand in mono- and disubstituted derivatives of the rhodium(II) acetate dimer.[4] Here we report the single-crystal X-ray structure of dichlorotris[2-(2-pyridyl)-1,8-naphthyridine]dirhodium(II) hexafluorophosphate acetonitrile solvate, $[Rh_2(pynp)_3Cl_2]$-

(1) The University of New South Wales.
(2) University of California.
(3) Binamira-Soriaga, E.; Sprouse, S. D.; Watts, R. J.; Kaska, W. C., submitted for publication.
(4) (a) Tikkanen, W. R.; Binamira-Soriaga, E.; Kaska, W. C.; Ford, P. C. *Inorg. Chem.* **1984**, *23*, 141–146. (b) Tikkanen, W. R., Binamira-Soriaga, E.; Kaska, W. C.; Ford, P. C. *Ibid.* **1983**, *22*, 1147–1148.

0020-1669/84/1323-3254$01.50/0

Table I

Crystal Parameters for $C_{41}H_{30}Cl_2F_{12}N_{10}P_2Rh_2$

cryst syst: triclinic	$\alpha = 73.49\ (1)^\circ$
space group: $P\bar{1}$	$\beta = 87.17\ (3)^\circ$
$a = 11.003\ (5)$ Å	$\gamma = 89.12\ (4)^\circ$
$b = 12.534\ (2)$ Å	$V = 2203\ (4)$ Å^3
$c = 16.685\ (2)$ Å	$Z = 2$

Data Collection

diffractometer: Enraf Nonius CAD4
radiation: Mo Kα (graphite monochromated, $\lambda = 0.710\ 73$ Å)
cryst dimens: 0.24 mm × 0.1 mm × 0.1 mm
linear abs coeff = 8.94 cm^{-1}
temp = 21 °C
$2\theta_{max} = 46.0$
no. of reflcns measd = 6485
no. of unique reflcns = 6107
no. of obsd reflcns ($I > 3.0\sigma(I)$) = 4603
$R = \Sigma||F_o| - |F_c||/\Sigma|F_o| = 0.0444$
$R_w = [\Sigma w_h||F_o| - |F_c||^2/\Sigma w_h|F_o|^2]^{1/2} = 0.0579$

$[PF_6]_2 \cdot CH_3CN$ (I), where both coordination modes are observed in the same complex: Two pynp ligands are tridentate and bridge the dirhodium(II) core via the naphthyridine fragment while the third pynp chelates a single rhodium atom via its bipyridine fragment.

Experimental Section

The pynp ligand was prepared as described by Caluwe.[5a] Dirhodium(II) tetraacetate was used as purchased from Strem Chemicals. Refluxing a 2/2/1 molar ratio of pynp/HCl(aq)/$Rh_2(O_2CCH_3)_4$ in degassed reagent grade methanol for 8 h gave a dark, air-stable solution, containing mono-, di-, and trisubstituted complexes. The ion $[Rh_2(pynp)_3Cl_2]^{2+}$ was isolated as the first dark brown band eluted with ethanol on a 1-m column of Sephadex LH-20 from the reaction solution. Addition of aqueous ammonium hexafluorophosphate (5% w/v) and reducing the volume gave a brown powder, which was collected by suction filtration. This material was recrystallized by slow evaporation of an acetonitrile/water (ca. 3/1) solution to give dark brown prisms suitable for X-ray structure determination (Table I).

The rhodium atoms were located by Patterson synthesis. The remaining non-hydrogen atoms of the complex cation and the two hexafluorophosphate anions were located by Fourier methods using data phased from partial structures. Scattering factors and anomalous dispersion corrections were taken from ref 5b. Anisotropic refinement reduced the value of R_1 to 0.11. A difference map then located an acetonitrile or crystallization. The inclusion of the CH_3CN in the calculation of density gave good agreement with experiment (d_{cacd} = 1.853 g/cm^3, d_{obsd} = 1.841 g/cm^3).

Final cycles of refinement used a restrained block-diagonal least-squares method (RAELS[6]). Restraints[7] were used to minimize differences in equivalent bond lengths within the three pynp ligands. Rigid-body thermal motion (TLX model[8]) was imposed on the individual ligands, the CH_3CN, and the anions. The rhodium and chlorine atoms were refined as isolated antisotropic atoms. The CH_3CN was restrained to be linear and the PF_6^- groups were restrained to be of D_{2h} symmetry by using local axial systems to describe geometry.[9]

Two of the three pynp ligands are tridentate, but the remaining ligand is bidentate. The N–C distances involving the uncoordinated nitrogen atom on the bidentate ligand were not restrained. These bond lengths refined to apparently shorter values than the corresponding bonds on the tridentate ligands, but this shortening was not significant at the 3σ level. Hydrogen atoms of the acetonitrile were excluded, but the other 27 hydrogen atoms were added in geometrically

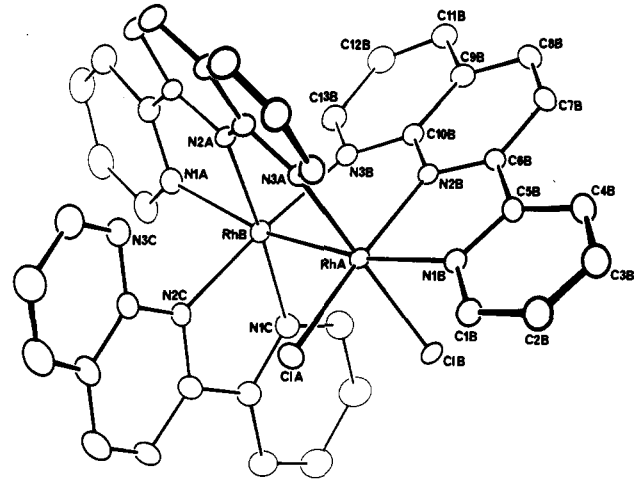

Figure 1. Perspective view and atom-labeling scheme for the cation of I.

sensible positions and restrained to move in conjunction with the positional shifts of the atoms to which these are attached. The structure contains 69 non-hydrogen atoms, and the restrained anisotropic refinement used 291 variable parameters in five blocks corresponding to 259 degrees of freedom. Positional coordinates are listed in Table II.

Results and Discussion

Figure 1 shows the structure and atom-labeling scheme for the $[Rh_2(pynp)_3Cl_2]^{2+}$ ion. The complex ion has two rhodium atoms joined by a bond of 2.5668 (7) Å and bridged by the naphthyridine fragments of two pynp ligands. The sites trans to the Rh–Rh bond are occupied by the pyridyl moieties of the bridging pynp ligands. Thus, nitrogens from the bridging pynp ligands occupy three coordination sites on each rhodium atom, and a fourth site is occupied by the rhodium–rhodium bond. Hexacoordination of the rhodium(II) centers is achieved at one rhodium by coordinating the bipyridyl fragment of the third pynp and at the other rhodium center by coordinating two chlorides. As a consequence, the dinuclear cation is quite asymmetric, in fact, chiral. Tables III and IV summarize some important bond lengths and bond angles, respectively.

The rhodium–rhodium bond length observed (2.567 Å) for I is comparable to but slightly shorter than that found for two other structurally characteruzed dirhodium(II) complexes with two bridging ligands, dichlorobis(μ-formato)bis(1,10-phenanthroline)dirhodium(II), $[Rh_2(phen)_2(\mu\text{-}HCO_2)_2Cl_2]$ (2.576 Å),[10] and bis(μ-acetato)bis(dimethylglyoxime)bis(triphenylphosphine)dirhodium(II), $[(Rh_2(dmg)_2(\mu\text{-}CH_3CO_2)_2(PPh_3)_2]$ (2.618 Å).[11] Predictably, the Rh–Rh bond of I is significantly longer than that in dirhodium(II) ions with four bridging ligands, e.g., $[Rh_2(\mu\text{-}CH_3CO_2)_4(py)_2]$ (2.396 Å)[12] and $[Rh_2(bpnp)(\mu\text{-}CH_3CO_2)_3]PF_6$ (2.405 Å; bpnp = 2,7-bis(2-pyridyl)-1,8-naphthyridine).[4]

The rhodium–nitrogen distances in I illustrate the trans influence of the rhodium–rhodium bond. The Rh–pyridyl nitrogen bonds RhB–N1A and RhB–N1B, which are trans to the Rh–Rh bond, have an average length of 2.175 (15) Å, much greater than that of the RhB–N1C bond (2.016 Å), which is cis to the Rh–Rh axis. Similarly the RhA–ClA and RhA–ClB bond lengths (2.34 and 2.36 Å, respectively) are ~0.15 Å shorter than those found in $[Rh_2(phen)_2(\mu\text{-}HCO_2)_2Cl_2]$, where the chlorides occupy sites trans to the Rh–Rh bond.[10]

Several other comparisons are of note. The RhB–N3C distance (3.29 Å) is too long to represent significant coordi-

(5) (a) Majewicz, T. G.; Caluwe, P. *J. Org. Chem.* **1979**, *44*, 531–535. (b) "International Tables for X-ray Crystallography"; Kynoch Press: Birmingham, England, 1974; Vol. 4.
(6) Rae, A. D. "RAELS: A Comprehensive Constrained Least-Squares Refinement Program", University of New South Wales, 1983.
(7) (a) Waser, J. *Acta Crystallgr.* **1963**, *16*, 1091–1094. (b) Rae, A. D. *Act Crystallogr., Sect. A* **1978**, *A34*, 578–582.
(8) (a) Schomaker, V.; Trueblood, K. N. *Acta Crystallogr., Sect. B* **1968**, *B24*, 63–76. (b) Rae, A. D. *Acta Crystallogr., Sect. A* **1975**, *A31*, 570–574.
(9) Rae, A. D. *Acta Crystallogr., Sect. A* **1975**, *A31*, 560–570.
(10) Pasternak, H.; Prochnik, F. *Inorg. Nucl. Chem. Lett.* **1976**, *12*, 591.
(11) Halpern, J.; Kimura, E.; Molin-Case, J.; Wong, C. S. *J. Chem. Soc. D* **1971**, 1207.
(12) Koh, Y. B.; Christoph, G. G. *Inorg. Chem.* **1979**, *18*, 1122–1128.

Table II. Positional Coordinates for $[Rh_2(pynp)_3Cl_2][PF_6]_2 \cdot CH_3CN$

atom	x	y	z
RhA	0.400 12 (4)	0.150 82 (4)	0.215 29 (3)
RhB	0.263 26 (4)	−0.021 40 (4)	0.267 70 (3)
ClA	0.413 00 (17)	0.197 60 (15)	0.340 96 (10)
ClB	0.586 09 (15)	0.051 94 (15)	0.232 13 (11)
N1A	0.112 47 (48)	−0.140 27 (44)	0.295 59 (33)
C1A	0.114 57 (68)	−0.251 33 (50)	0.333 77 (45)
C2A	0.017 30 (70)	−0.317 31 (68)	0.332 89 (52)
C3A	−0.084 51 (77)	−0.270 95 (66)	0.289 95 (52)
C4A	−0.089 86 (64)	−0.158 03 (64)	0.254 96 (48)
C5A	0.010 64 (53)	−0.094 47 (49)	0.258 68 (42)
C6A	0.012 74 (48)	0.027 83 (49)	0.226 86 (42)
C7A	−0.095 16 (57)	0.090 22 (61)	0.208 45 (48)
C8A	−0.091 45 (59)	0.202 26 (62)	0.189 28 (52)
C9A	0.019 68 (53)	0.257 24 (54)	0.185 62 (48)
C10A	0.125 25 (48)	0.191 94 (45)	0.201 33 (41)
N2A	0.120 75 (42)	0.077 98 (40)	0.222 52 (31)
C11A	0.030 50 (70)	0.372 94 (57)	0.170 36 (55)
C12A	0.141 46 (63)	0.41764 (62)	0.170 83 (52)
C13A	0.242 83 (63)	0.348 13 (50)	0.184 93 (44)
N3A	0.238 09 (44)	0.237 85 (42)	0.198 80 (32)
N1B	0.509 55 (47)	0.291 39 (43)	0.145 72 (29)
C1B	0.573 80 (60)	0.362 41 (52)	0.175 42 (43)
C2B	0.651 97 (71)	0.439 71 (62)	0.125 52 (45)
C3B	0.668 75 (76)	0.443 57 (67)	0.041 83 (46)
C4B	0.603 61 (66)	0.372 84 (59)	0.011 15 (44)
C5B	0.524 79 (59)	0.296 12 (52)	0.064 23 (34)
C6B	0.456 72 (56)	0.211 75 (49)	0.038 43 (32)
C7B	0.454 92 (64)	0.210 27 (60)	−0.045 62 (35)
C8B	0.399 19 (63)	0.127 12 (58)	−0.066 17 (40)
C9B	0.343 74 (61)	0.040 79 (55)	−0.002 88 (34)
C10B	0.342 61 (54)	0.046 90 (48)	0.079 83 (32)
N2B	0.397 38 (43)	0.133 46 (39)	0.099 06 (29)
C11B	0.287 35 (65)	−0.049 96 (59)	−0.019 57 (45)
C12B	0.239 92 (70)	−0.131 74 (64)	0.045 35 (41)
C13B	0.240 66 (62)	−0.120 03 (56)	0.125 84 (41)
N3B	0.288 83 (46)	−0.033 63 (42)	0.144 98 (31)
N1C	0.395 00 (49)	−0.129 84 (43)	0.318 09 (30)
C1C	0.459 98 (65)	−0.194 40 (57)	0.278 65 (45)
C2C	0.548 88 (76)	−0.265 66 (69)	0.316 56 (49)
C3C	0.573 72 (79)	−0.274 92 (70)	0.398 82 (48)
C4C	0.508 21 (64)	−0.210 68 (58)	0.439 48 (46)
C5C	0.418 31 (57)	−0.140 37 (52)	0.398 38 (35)
C6C	0.339 42 (55)	−0.071 65 (52)	0.437 82 (34)
C7C	0.354 46 (70)	−0.069 18 (62)	0.520 64 (36)
C8C	0.282 58 (71)	−0.003 49 (67)	0.554 23 (45)
C9C	0.193 61 (72)	0.061 27 (66)	0.505 22 (40)
C10C	0.177 34 (63)	0.052 54 (58)	0.424 45 (38)
N2C	0.252 80 (44)	−0.012 84 (42)	0.390 40 (31)
C11C	0.118 56 (87)	0.136 38 (78)	0.532 93 (54)
C12C	0.031 42 (91)	0.193 58 (87)	0.483 74 (52)
C13C	0.017 38 (82)	0.173 19 (78)	0.406 93 (49)
N3C	0.088 82 (56)	0.106 24 (53)	0.377 30 (38)
H1A	0.188 27 (68)	−0.285 82 (50)	0.363 67 (45)
H2A	0.020 56 (70)	−0.399 37 (68)	0.360 06 (52)
H3A	−0.156 60 (77)	−0.317 85 (66)	0.288 45 (52)
H4A	−0.163 57 (64)	−0.123 55 (64)	0.225 06 (48)
H7A	−0.175 04 (57)	0.052 15 (61)	0.210 92 (48)
H8A	−0.167 93 (59)	0.246 86 (62)	0.177 05 (52)
H11A	−0.043 09 (70)	0.421 91 (57)	0.160 55 (55)
H12A	0.147 41 (63)	0.500 26 (62)	0.158 96 (52)
H13A	0.325 03 (63)	0.381 35 (50)	0.184 35 (44)
H1B	0.562 53 (60)	0.358 73 (52)	0.235 98 (43)
H2B	0.697 40 (71)	0.492 27 (62)	0.148 33 (45)
H3B	0.725 31 (76)	0.498 94 (67)	0.003 46 (46)
H4B	0.614 87 (66)	0.376 51 (59)	−0.049 42 (44)
H7B	0.495 62 (64)	0.269 76 (60)	−0.091 82 (35)
H8B	0.399 90 (63)	0.123 50 (58)	−0.125 30 (40)
H11B	0.286 42 (65)	−0.055 66 (59)	−0.078 12 (45)
H12B	0.202 48 (70)	−0.196 87 (64)	0.032 54 (41)
H13B	0.203 26 (62)	−0.179 63 (56)	0.173 54 (41)
H1C	0.442 16 (65)	−0.188 52 (57)	0.219 35 (45)
H2C	0.596 82 (76)	−0.312 85 (69)	0.287 08 (49)
H3C	0.637 56 (79)	−0.326 71 (70)	0.428 70 (48)
H4C	0.526 02 (64)	−0.216 55 (58)	0.498 78 (46)
H7C	0.418 81 (70)	−0.113 32 (62)	0.556 05 (36)
H8C	0.293 34 (71)	−0.000 40 (67)	0.612 69 (45)
H11C	0.129 71 (87)	0.146 67 (78)	0.589 39 (54)
H12C	−0.020 79 (91)	0.244 41 (87)	0.507 35 (52)
H13C	−0.047 55 (82)	0.213 91 (78)	0.370 24 (49)
PA	−0.080 18 (17)	−0.290 33 (16)	0.058 55 (11)
F1A	−0.172 91 (38)	−0.264 06 (44)	−0.011 83 (26)
F3A	0.023 44 (41)	−0.280 00 (62)	−0.006 42 (29)
F2A	−0.089 79 (55)	−0.409 50 (45)	0.066 15 (41)
F4A	0.012 54 (39)	−0.316 60 (44)	0.128 94 (27)
F5A	−0.183 81 (42)	−0.300 66 (63)	0.123 53 (29)
F6A	−0.070 58 (55)	−0.171 16 (45)	0.050 95 (40)
PB	0.750 42 (20)	0.420 52 (17)	0.395 96 (14)
F1B	0.883 75 (47)	0.422 13 (41)	0.369 44 (31)
F2B	0.776 88 (45)	0.333 40 (41)	0.480 15 (34)
F3B	0.729 31 (56)	0.327 06 (43)	0.356 70 (36)
F4B	0.617 09 (50)	0.418 91 (45)	0.422 48 (35)
F5B	0.723 96 (44)	0.507 64 (41)	0.311 77 (34)
F6B	0.771 53 (53)	0.513 98 (43)	0.435 22 (34)
CA	0.651 01 (59)	0.458 63 (64)	0.718 04 (71)
CB	0.666 03 (117)	0.525 63 (94)	0.631 21 (75)
N	0.639 15 (82)	0.405 75 (69)	0.786 58 (59)

Table III. Bond Lengths in the Cation of I (Å)

RhA-RhB	2.5668 (7)	RhB-N1A	2.190 (5)
RhA-ClA	2.343 (2)	RhB-N2A	2.025 (5)
RhA-ClB	2.363 (2)	RhB-N3B	2.101 (5)
RhA-N3A	2.065 (5)	RhB-N1C	2.016 (5)
RhA-N1B	2.160 (5)	RhB-N2C	2.078 (5)
RhA-N2B	2.014 (5)		

Table IV. Bond Angles in the Cation of I (deg)

angles around RhA		angles around RhB	
RhB-RhA-ClA	99.13 (5)	RhA-RhB-N1A	165.8 (1)
-ClB	95.80 (5)	-N2A	87.8 (1)
-N3A	84.5 (1)	-N3B	84.6 (1)
-N1B	168.0 (1)	-N1C	96.8 (2)
-N2B	88.8 (1)	-N2C	93.7 (1)
ClA-RhA-ClB	93.2 (1)	N1A-RhB-N2A	78.2 (2)
-N3A	87.5 (2)	-N3B	92.2 (2)
-N1B	92.7 (1)	-N1C	97.3 (2)
-N2B	171.6 (1)	-N2C	90.5 (2)
ClB-RhA-N3A	179.2 (2)	N2A-RhB-N3B	84.9 (2)
-N1B	85.1 (2)	-N1C	175.2 (2)
-N2B	88.5 (1)	-N2C	99.4 (2)
N3A-RhA-N1B	94.4 (2)	N3B-RhB-N1C	96.7 (2)
-N2B	90.8 (2)	-N2C	175.3 (2)
N1B-RhA-N2B	79.2 (2)	N1C-RhB-N2C	79.1 (2)

nation of the N3C atom. The RhA–N3A and RhB–N3B distances for the bridging ligands are more than 1 Å shorter. The differences between the bridging and chelating pynp ligands are also reflected in the coordinate bond distances to the middle nitrogen or these ligands. The RhB–N2C bond is >0.05 Å longer than the analogous RhB–N2A and RhA–N2B bonds. Lastly, there are interesting differences in the bond lengths between the bridging pynp ligands and the two metal centers. Comparisons of analogous bonds, e.g. RhA–N3A vs. RhB–N3B, show in each case the bond to RhA to be the shorter. Given that RhA should be the less positive metal center owing to the coordination also of the two chlorides, the opposite might have been expected. The probable explanation of the bond length differences very likely lies in the greater steric crowding around RhB.

Acknowledgment. We acknowledge the U.S. Department of Energy (P.C.F.) and the Army Research Office, Durham (W.C.K.), for partial support.

Registry No. I, 91210-87-6; $Rh_2(O_2CCH_3)_4$, 15956-28-2; Rh, 7440-16-6.

Supplementary Material Available: Listings of comprehensive structural details, thermal parameters for all atoms, and observed and calculated structure factors (24 pages). Ordering information is given on any current masthead page.